Tectonophysics 661 (2015) 210–214

Contents lists available at ScienceDirect

Tectonophysics

journal homepage: www.elsevier.com/locate/tecto

Is the Lishan fault of Taiwan active?

Hao Kuo-Chen [a,*], Francis Wu [b,c], Wu-Lung Chang [a], Chih-Yu Chang [a], Ching-Yu Cheng [a], Naoshi Hirata [d]

[a] Department of Earth Sciences, National Central University, Jhongli, Taiwan
[b] Department of Geological and Environmental Sciences, State University of New York at Binghamton, Binghamton, USA
[c] Department of Earth Sciences, University of Southern California, Los Angeles, USA
[d] Earthquake Prediction Research Center, Tokyo University, Tokyo, Japan

ARTICLE INFO

Article history:
Received 16 June 2015
Received in revised form 1 September 2015
Accepted 2 September 2015
Available online 12 September 2015

Keywords:
Lishan fault
Focal mechanism
Ductile shear zone
Active fault zone
Dense seismic array

ABSTRACT

The Lishan fault has been characterized alternately as a major discontinuity in stratigraphy, structures and metamorphism, a ductile shear zone, a tectonic suture or non-existent. In addition to being a geological boundary, it also marks transitions in subsurface structures. Thus, the seismicity to the west of the fault permeates through the upper and mid-crust while beneath the Central Range it is noticeably less and largely concentrated in the upper 12 km. A prominent west-dipping conductive zone extends upward to meet the Lishan fault. Also, the eastward increase of crust thickness from ~30 km in the Taiwan Strait quickens under the Lishan fault to form a root of over 50 km under the Central Range. In the past, the small magnitude seismicity along the Lishan fault has been noticed but is too diffuse for definitive association with the fault. Recent processing of aftershock records of the 1999 Mw 7.6 Chi-Chi earthquake using Central Weather Bureau data and, especially, data from three post-Chi-Chi deployments of seismic stations across central Taiwan yielded hypocenters that appear to link directly to the Lishan structure. The presence of a near 4-km-long vertical seismic zone directly under the surface trace of the Lishan fault indicates that it is an active structure from the surface down to about 35 km, and the variety of focal mechanisms indicates that the fault motion can be complex and depth-dependent.

1. Introduction

The Lishan fault of Taiwan as described in Tsan (1971) and Biq (1971) is the eastern boundary of the Hsuehshan Range and follows a topographically prominent valley that runs from the western apex of the Ilan Plain to central Taiwan for a distance of about 200 km (Fig. 1a). The fault was interpreted as an oblique left-lateral shear zone (Biq, 1971) and a major structural and stratigraphic boundary (Ho, 1975; Tsan, 1971) that separates two of the main mountain ranges in northern Taiwan, the Hsuehshan and the Backbone Ranges (Fig. 1a). Teng et al. (1991), Lee et al. (1997) and Brown et al. (2012) tied it to Paleogene normal faulting on the continental margin that subsequently was inverted after the collision of the Eurasian and Philippine Sea plates began. But Lu and Hsu (1992) and Huang et al. (1997) interpreted it to be a suture between the continental margin and the late-Miocene accretionary prism. Field evidence led Lee et al. (1997) to argue that reverse sinistral high-angle fault slips took place during late Cenozoic era, with extension at the northeastern end of the fault owing to the opening of the Okinawa Trough. Brown et al. (2012) viewed the fault as the backstop for the detachment below the fold-and-thrust belt of western Taiwan. Brown et al. (2012) emphasized the presence of ductile nature of the fault. However, lack of observable displacement in schistose strata across the presumed fault led to its deletion in the current Geologic Map of Taiwan (Chen et al., 2000).

As the subsurface information gathered, the Lishan fault zone has been noticed as a clear but rather diffuse boundary (Bertrand et al., 2009, 2012; Wu, 1978; Wu et al., 2004). For example, seismicity disseminates through the mid-crust west of a west-dipping, high conductivity zone beneath the fault (Bertrand et al., 2009, 2012) (Fig. 1b and d), where this zone is also in the vicinity where the lower crust of the seismic velocity structures (6.5–7.5 km/s) transits from gentle flexure to its west to significant thickening under the high ranges to the east (e.g., Kuo-Chen et al., 2012; Wu et al., 2014) (Fig. 1c).

The Lishan fault may or may not lead to major seismic hazards, but the ample seismicity in its vicinity can be used to assess whether the Lishan fault is active and what is the possible fault kinematics. In this paper, we combine data from CWB with data acquired during three deployments by the Earthquake Research Institute (ERI), University of Tokyo, in 1999, 2001 and 2005 across central Taiwan after the 1999 Chi-Chi earthquake (Fig. 1a). In particular, stations in the dense linear array of 2001 provided data to locate precisely a cluster of events near the Lishan fault. These new results prompted us to reexamine previously determined seismicity and focal mechanisms and sketch out a consistent vertically contiguous zone of activity. The different kinematics at different depth however depicts a relatively complex mode of deformation along the Lishan boundary.

* Corresponding author at: Dept. of Earth Sciences, National Central University, No. 300, Jhongda Rd., Jhongli City, Taoyuan County 32001, Taiwan. Tel.: +886 3 422 7151x65602; fax: +886 3 422 2044.
E-mail address: kuochen@ncu.edu.tw (H. Kuo-Chen).

http://dx.doi.org/10.1016/j.tecto.2015.09.002
0040-1951/

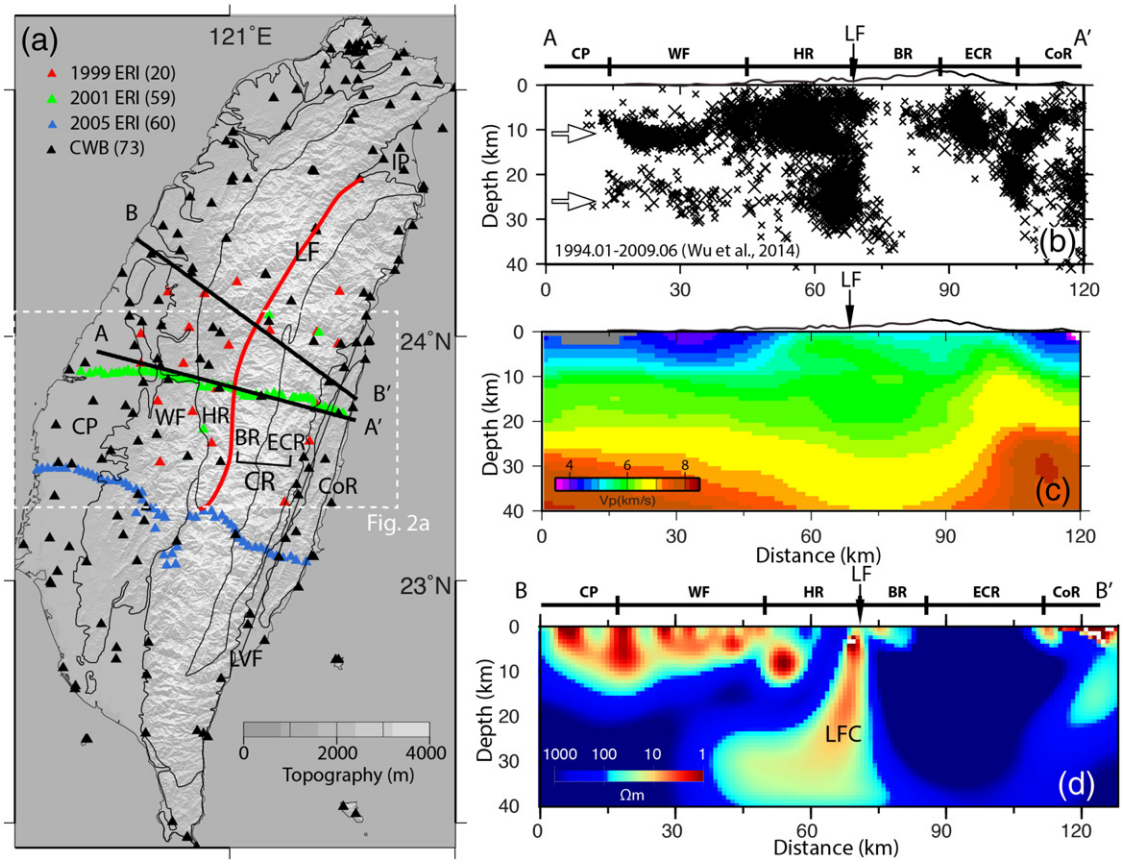

Fig. 1. (a) Geological provinces of Taiwan and the seismic networks of CWB (Central Weather Bureau) and ERI (Earth Research Institute of Tokyo University). IP: Ilan Plain, CP: Coastal Plain, WF: Western Foothills, HR: Hsuehshan Range, BR: Backbone Range (Western Central Range), ECR: Eastern Central Range, CoR: Costal Range. LF: Lishan fault, LVF: Longitudinal Valley Fault. White-dashed rectangular area: the study region. (b) Seismicity profile A–A′ after hypoDD relocation in central Taiwan from Wu et al. (2014). Two horizontal white arrows: double-layered seismicity. (c) Seismic Vp profile A–A′ from Kuo-Chen et al. (2012). (d) Resistivity profile B–B′ from Bertrand et al. (2009).

2. Tectonic framework of central Taiwan

In this section, we briefly describe the key geologic elements relevant to our ensuing discussion of the Lishan fault. The main geologic/tectonic units of Taiwan are shown in Fig. 1a and its captions. The Lishan fault is bounded on the east by the Miocene slaty rocks of the Backbone Range, the Lushan formation, and the Eocene–Oligocene rocks of higher metamorphic grade of the Hsuehshan Range on the west side. Field evidence shows that the Lushan formation is relatively thin (a few kilometers) and below it lies the Pre-Tertiary Taroko formation, with schists and other metamorphic rocks (Lee et al., 1997; Brown et al., 2012).

Near the surface, rocks in the Hsuehshan Range are recognized as composed of Eocene–Oligocene continental shelf sediments, whereas on the Backbone Range side Miocene pelitic sediments are found (Lee et al., 1997; Lin et al., 2003) and the rocks of the Taroko formation in the Eastern Central Range are pre-Mesozoic in age and likely to have been rooted in the lower crust (Jahn et al., 1976). The Lishan fault may have its origin as a normal fault when the Eurasian margin underwent extension, and had inverted subsequently (Brown et al., 2012; Lester et al., 2012) and contributed to the overall uplift of the Central Range.

3. Seismicity and focal mechanisms associated with the Lishan fault

3.1. Combined ERI and CWB data

The 1999 Chi-Chi earthquakes produced an extensive series of aftershocks. The CWB seismic networks cover the period before and after the earthquake. In addition, one month after the mainshock, ERI deployed 20 temporary seismic stations in central Taiwan to record aftershocks for three months (October to December). Then in 2001 (March to May) and 2005 (March to April), two east–west trended linear arrays of 59 and 60 stations, respectively, were installed across central and southern Taiwan (Fig. 1a), primarily to explore crustal structures. We picked 19,172 P-wave first arrivals from the ERI data and used an additional 22,813 arrivals from the Central Weather Bureau (CWB) catalog to locate a total of 972 earthquakes. Benefited by the dense stations in the temporary seismic array, we were able to obtain as many as 27 arrivals for the smallest earthquake (M_L 1.2). The initial hypocenters, based on the 1D velocity model of Chen (1995), were relocated using hypoDD (Waldhauser and Ellsworth, 2000) in order to enhance clustering.

The results of the hypoDD location show several previously recognized earthquake clusters (Fig. 2a and b) (e.g., Kao and Chen, 2000 and Wu et al., 2004). However, a new narrow, steeply dipping zone of seismicity near the Lishan fault is found amid several known clusters (Fig. 2a–c). This zone of 114 events was recorded in 2001, dipping steeply to the west within a depth range of 0–14 km (Fig. 2b). The epicenters form a narrow, ~4 km-long NW trending band intersecting with the mapped fault trace (Fig. 2c).

The combined 2001 ERI and CWB data enable us to determine the focal mechanisms of two of the largest earthquakes in 2001, with M_L of 3.5 and 3.0, using P-wave polarities and the FOCMEC code (Snoke et al., 1984). Both solutions are well constrained and show similar left-lateral strike-slip motion (the average parameters are: Strike: 143°, Dip: 76°, Rake: −11°) (Fig. 2c and d).

3.2. Seismicity along Lishan fault based on 1994–2009 CWB catalog

With average station spacing on the order of 20 to 30 km, the upgraded CWB network seismicity had been studied by Wu et al.

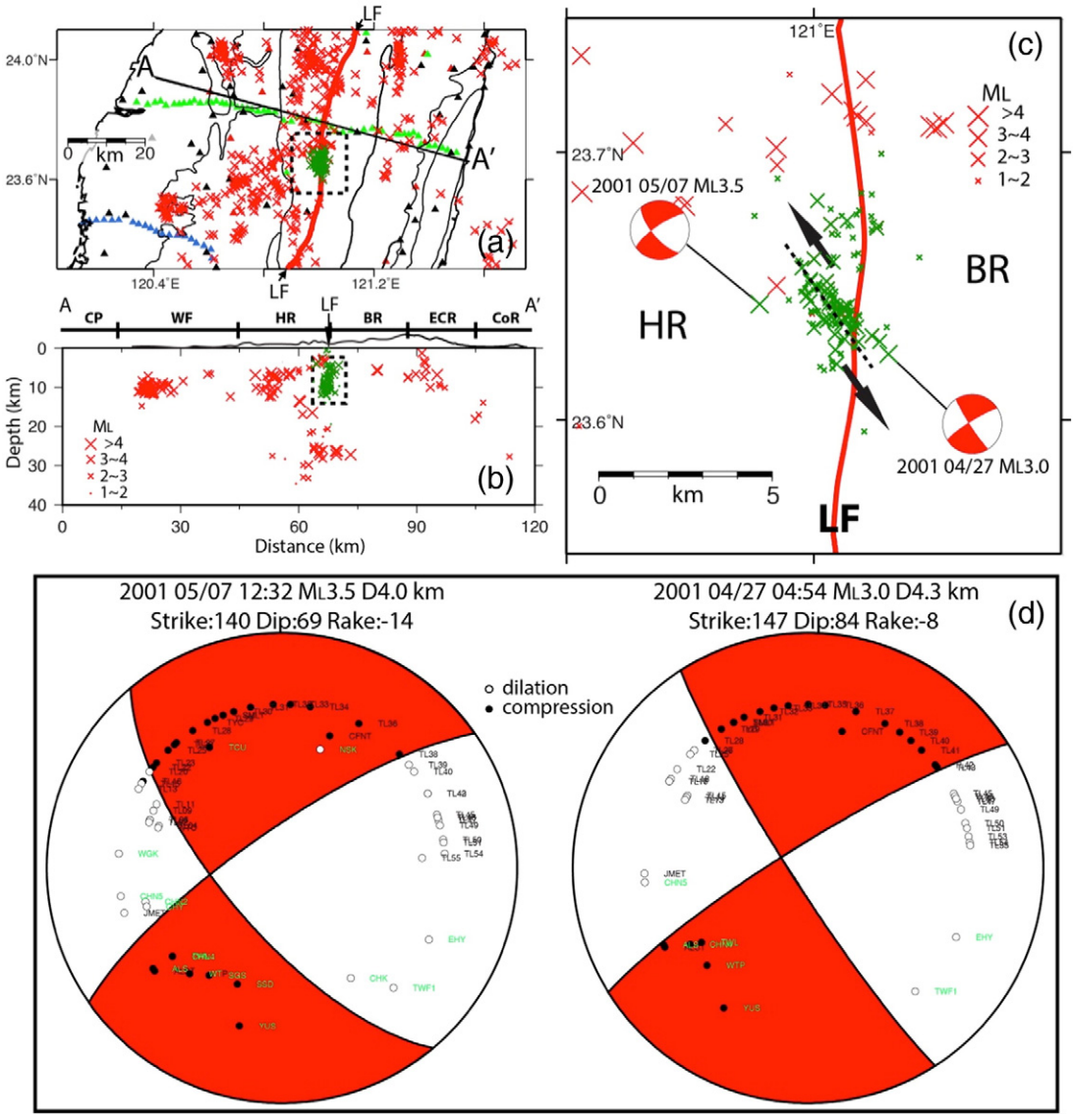

Fig. 2. (a) Map view of seismicity. Seismicity after hypoDD relocation in central Taiwan from this study (red crosshairs). A new cluster of seismicity identified near the Lishan fault zones: green crosshairs. Black lines: geological boundaries (see Fig. 1a). Red line: the Lishan fault. Red crosshair: seismicity in this study. Black-dashed rectangular area: the selected region in Fig. 2c. (b) Seismicity profile A–A′ after hypoDD relocation in central Taiwan from this study. Black-dashed rectangular area: a new cluster of seismicity identified in this study (green crosshairs). (c) Map view of the seismicity and focal mechanisms in this study. A left-lateral vertical dipping fault zone of seismicity corresponds to the focal mechanisms. Red crosshair: seismicity in this study. (d) Two focal mechanisms determined by using P wave first polarities. Circles with green-color labels: P wave first polarities with station names from CWB. Black circles with station names: P wave first polarities from ERI. Open circles: dilation. Black circle: compression.

(2004, 2014) and Brown et al. (2012) among others. Although a direct link of hypocenters to the fault was not warranted even after hypoDD relocation, it is clear that the overall seismicity patterns differ significantly on the two sides of the fault (Fig. 3a). To the west distinctive double-layered seismicity (~10 km and ~30 km depths) is found under the Hsuehshan Range and the Coastal Plain, for which Wu et al. (2004, 2014) interpreted it in terms of the rheology of a continental crust (Chen and Molnar, 1983). Across the fault to the east, in contrast, the seismicity under the Central Range is either limited to shallow depth (<12 km) or almost completely absent.

Fig. 3b shows focal mechanisms of 14 events located close to the fault from the Broad Array for Taiwan Seismology database (BATS; http://bats.earth.sinica.edu.tw), of which seven events have one of the planes parallel or sub-parallel to the Lishan fault and are dominantly left-lateral strike-slip solutions. The other solutions include two thrust fault solutions with left-lateral motions on the N–S oriented planes, two dominant EW thrusts, and two low-angle/high-angle thrust motions. The depths of these events are all above 12 km (Fig. 3b and Table 1) and the averaged P-axis (σ_1) and T-axis (σ_3) are 308° and 209°, respectively (Fig. 3c). In central Taiwan, on the other hand, a steeply westward dipping seismic zone between ~14–35 km (Fig. 3a) became clear especially after the 1999 Chi-Chi earthquake (Wu et al., 2004, 2014). The focal mechanisms of M > 4.5 events in this zone are mostly thrusts, with one high (>70°) and one low angle plane, with P-axes perpendicular to the main trend of Taiwan. These observations thus suggest that fault motions appear to be depth-dependent across the Lishan fault.

4. Discussion and conclusion

We are able to lower the magnitude threshold and obtain precisely located seismicity along part of the Lishan fault in central Taiwan by combining P picks from CWB permanent and temporary ERI networks. The dense linear array deployed in 2001 by ERI, in particular, provides

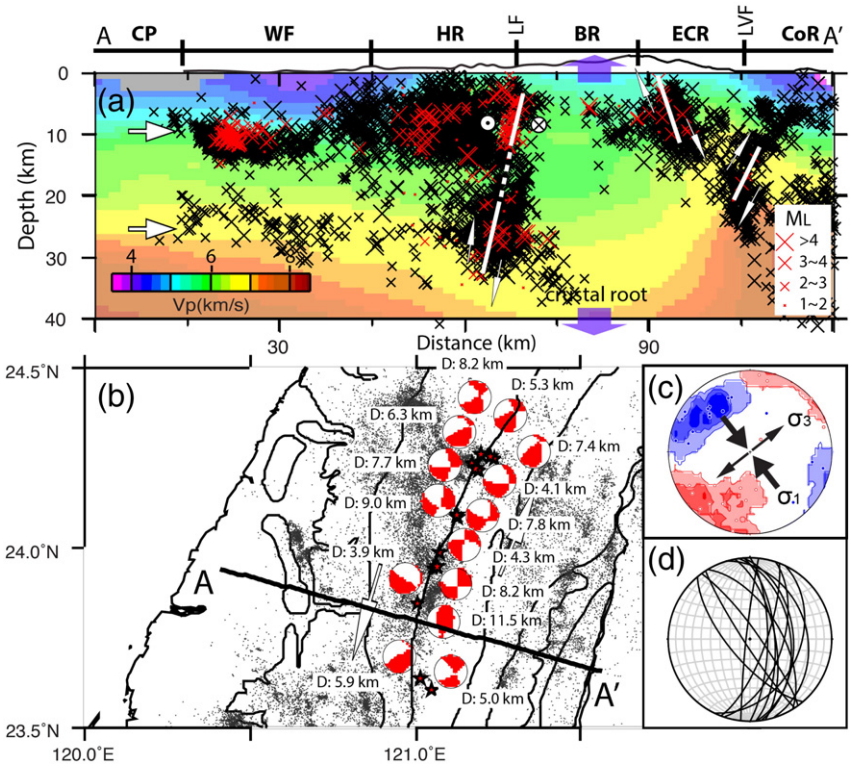

Fig. 3. (a) Seismicity from Wu et al. (2004) (black crosshairs) and this study (red crosshairs), and P wave velocity profile (Kuo-Chen et al., 2012) along A–A′ in Fig. 3(b). Two horizontal white arrows: double-layered seismicity. White solid lines with white arrows: fault zones with their motions based on the focal mechanisms from Wu et al. (2014) and this study. Thick purple arrows: the crustal movement of the Central Range. (b) Focal mechanisms near the Lishan fault zone from Broadband array in Taiwan for Seismology (BATS) (Table 1). (c) Contour of P- and T-axes obtained from the focal mechanisms in Figs. 2c and 3a. P-axis (σ_1): blue circle. T-axis (σ_3): red circle. (d) The strikes of 14 fault planes sub-parallel to the main Lishan fault trace.

key data to the mapping of a well-defined seismic zone near the Lishan fault from near surface to about 14 km. The epicentral distribution of the cluster does not align with the Lishan fault presented in geologic maps (e.g., Lee et al., 1997) but at an angle of about 40°, and one of the planes of both focal mechanisms of two larger events is nearly parallel to the strike of the seismic zone. It is interesting that faults with similar orientations and directions of motion were mapped by Lee (1995). Focal mechanisms of large events recorded by BATS in the vicinity of the Lishan fault (Fig. 3b and Table 1) also show off-trend fault planes. Judging from the seismicity around the mapped fault, detailed geologic studies by Lee et al. (1997) indicate that the foliations, joints, and fractures vary significantly in their orientations and the Lishan fault may have a "polyphase" history.

That the seismic zone in Fig. 2c and one of the planes of a majority (12 of 14) of the focal mechanisms in Fig. 3d are sub-parallel to the main fault zone suggest that the main fault and the active subsidiary faults can perhaps be interpreted as synthetic members of a Riedel system (Riedel, 1929). The strikes of these planes with respect to the main Lishan trace are, however, somewhat larger than the range of 10–20° often cited for Riedel faults (Twiss and Moore, 1992). The P- and T-axes for the focal mechanisms presented can be used to define an average direction of these axes as shown in Fig. 3c. As the majority of events are in northern Taiwan, the stress axes are rotated clockwise with respect to those of central Taiwan, reflecting the changes in collision geometry along the trend of Taiwan (Wu et al., 2009). Judging from small-scale brittle and ductile structures (Lee, 1995; see Fig. 16 in the paper) both the Riedel R and P faults are found in the Lishan fault zone.

From short-term and long-term rates of uplift (Ching et al., 2011; Lee et al., 2006), the Central Range is rising faster than the Hsuehshan

Table 1
Focal mechanisms near Lishan fault. Focal mechanisms are from BATS. Earthquake locations are relocated by hypoDD (Wu et al., 2014).

Longitude	Latitude	Depth (km)	Strike	Dip	Rake	M_L	YYYYMMDDHHMN
121.191	24.2145	4.1	354.84	45.77	−16.04	4.5	199909210331
121.2385	24.2482	6.3	351.72	48.75	38.15	4.44	199909250419
121.1701	24.2369	7.4	342.75	30.86	6.93	4.38	199909250613
121.2252	24.2514	5.3	348.96	64.8	17.1	4.65	199909270403
121.1965	24.258	8.2	328.44	59.45	−7.65	4.68	199909270411
121.0477	23.6063	5.0	58.08	64.48	−170.07	3.84	199909280001
121.0057	23.8469	11.5	25.06	38.61	112.95	4.47	199910051218
121.0723	23.9864	4.3	278.18	65.08	−175.37	4.13	200001302021
121.1257	24.0842	7.8	18.03	56.74	−10.26	4.77	200009010924
121.1249	24.0901	9.0	118.33	65.5	−162.48	4.2	200012221123
121.0531	23.9442	8.2	19.97	12.89	−15.85	4.07	200105131457
121.0144	23.6368	5.9	357.42	21.78	29.76	4.41	200203181638
121.0646	23.9454	3.9	96.49	71.09	−161.46	3.52	200203231853
121.1809	24.2185	7.7	355.63	65.16	−13.49	4.14	200112281040

Range, thus the Lishan fault should have a vertical component as well, with the Central Range side up. But the Lishan structure does not behave uniformly throughout the crust, despite it is possible associated with a continuous high electrical conductivity zone from the surface to the lower crust as shown in Fig. 1d (Bertrand et al., 2009, 2012). In the upper crust (0–14 km) left-lateral motions on NW–SE striking planes seem to dominate as discussed above, while in the mid to lower crust (14–35 km) the high-angle west-dipping thrusts, at least in central Taiwan, imply the Central Range-down motion (Fig. 3a) (Wu et al., 2004). Thus, the shallow and deep parts of the Lishan fault show, respectively, the effects of oblique convergence at the upper crust and root building in the mid to lower crust.

We demonstrate in this study that data from a temporary dense seismic array, albeit not particularly designed for earthquake recording, in combination with the CWB data can contribute to mapping the subsurface extent and assessing the active status of the Lishan structures. Combined with seismicity from previous studies, seismic velocity structures, and resistivity profile, we conclude that this fault zone extends from the surface down to 35 km depth and is still active. Although it is not possible to assess now whether or not the Lishan fault may present a seismic hazard along its entire 200 km length, its deep part did generate a M_L 6.4 Chi-Chi aftershock and the neighboring faults apparently generated two $M_L > 6$ Nantou earthquakes in 2013 based on waveform modeling (Lee et al., 2015). With the micro-seismicity so high in Taiwan, many of the subsurface (blind) faults can be detected by precisely locating the micro-earthquakes. To do this, deployment of dense seismic network would be the key as shown in our study.

Acknowledgments

H. K-C was supported by National Science Council (Grant No.: NSC 101-2116-M-008-023-MY3) and Ministry of Science and Technology (Grant No.: MOST 104-2628-M-008-005-MY3). F. T. Wu was supported by US NSF (Grant No.: EAR 1010645). Discussions with Dr. Y. H. Lee of National Chung Cheng University are acknowledged. The calculation of contour of P- and T-axes in Fig. 3c is from the FaultKin7 software (http://www.geo.cornell.edu/geology/faculty/RWA/programs/faultkin.html). We thank the anonymous reviewer and Dennis Brown for their insightful detailed comments that helped us improve the manuscript.

References

Bertrand, E., Unsworth, M., Chiang, C.W., Chen, C.S., Chen, C.C., Wu, F., Türkoglu, E., Hsu, H.L., Hill, G., 2009. Magnetotelluric evidence for thick-skinned tectonics in central Taiwan. Geology 37 (8), 711–714. http://dx.doi.org/10.1130/ G25755A.1.

Bertrand, E., Unsworth, M., Chiang, C.W., Chen, C.S., Chen, C.C., Wu, F., Türkoglu, E., Hsu, H.L., Hill, G., 2012. Magnetotelluric imaging beneath the Taiwan orogen: an arc–continent collision. J. Geophys. Res. 117, B1. http://dx.doi.org/10.1029/2011JB008688.

Biq, C., 1971. Some aspects of post-orogenic block tectonics in Taiwan-recent crustal movement. R. Soc. N. Z. Bull. 9, 19–24.

Brown, D., Alvarez-Marron, J., Schimmel, M., Wu, Y.-M., Camanni, G., 2012. The structure and kinematics of the central Taiwan mountain belt derived from geological and seismicity data. Tectonics 31. http://dx.doi.org/10.1029/2012TC003156.

Chen, Y.-L., 1995. Three Dimensional Velocity Structure and Kinematic Analysis in Taiwan Area M.S. thesis Inst. of Geophys., Natl. Cent. Univ, Chung-Li, Taiwan.

Chen, W.-P., Molnar, P., 1983. Focal depths of intracontinental and intraplate earthquakes and their implications for the thermal and mechanical properties of the lithosphere. J. Geophys. Res. 88 (B5), 4183–4214. http://dx.doi.org/10.1029/JB088iB05p04183.

Chen, C.-H., et al. (2000), Geological map of Taiwan, scale 1:500,000, Cent. Geol. Sur., Taipei.

Ching, K.-E., Hsieh, M.-L., Johnson, K.M., Chen, K.-H., Rau, R.-J., Yang, M., 2011. Modern vertical deformation rates and mountain building in Taiwan from precise leveling and continuous GPS observations, 2000–2008. J. Geophys. Res. 116, B08406. http://dx.doi.org/10.1029/2011JB008242.

Ho, C.S., 1975. An introduction to the geology of Taiwan. Explanatory Text of the Tectonic Map of Taiwan. Ministry of Economic Affairs (126 pp.).

Huang, C.-Y., Wu, W.-Y., Chang, C.-P., Tsao, S., Yuan, P.-B., Lin, C.-W., Xia, K.-Y., 1997. Tectonic evolution of accretionary prism in the arc–continent collision terrane of Taiwan. Tectonophysics 281, 31–51. http://dx.doi.org/10.1016/S0040-1951(97)00157-1.

Jahn, B.M., Chen, P.Y., Yen, T.P., 1976. Rb–Sr ages of granitic rocks in southeastern China and their tectonic significance. Bull. Seismol. Soc. Am. 86, 763–776.

Kao, H., Chen, W.-P., 2000. The Chi-Chi earthquake sequence: active, out-of-sequence thrust faulting in Taiwan. Science 288, 2346–2349.

Kuo-Chen, H., Wu, F.T., Roecker, S.W., 2012. Three-dimensional P velocity structures of the lithosphere beneath Taiwan from the analysis of TAIGER and related seismic datasets. J. Geophys. Res. 117, B06306. http://dx.doi.org/10.1029/2011JB009108.

Lee, Y.-H., 1995. A study of the stress field system evolution of the Taiwan mountain belt, central cross-island highway and surrounding regions. Bull. Cent. Geol. Surv. 10, 51–90.

Lee, J.C., Angelier, J., Chu, H.-T., 1997. Polyphase history and kinematics of a complex major fault zone in the northern Taiwan mountain belt: The Lishan fault. Tectonophysics 274, 97–115. http://dx.doi.org/10.1016/S0040-1951(96)00300-9.

Lee, Y.H., Chen, C.C., Liu, T.K., Ho, H.C., Lu, H.Y., Lo, W., 2006. Mountain building mechanisms in the Southern Central Range of the Taiwan Orogenic Belt — from accretionary wedge deformation to arc–continental collision. Earth Planet. Sci. Lett. 252, 413–422.

Lee, S.-J., Yeh, T.-Y., Huang, H.-H., Lin, C.-H., 2015. Numerical earthquake models of the 2013 Nantou, Taiwan, earthquake series: characteristics of source rupture processes, strong ground motions and their tectonic implication. J. Asian Earth Sci. http://dx.doi.org/10.1016/j.jseaes.2015.06.031.

Lester, R., Lavier, L.L., McIntosh, K., Van Avendonk, H.J.A., Wu, F., 2012. Active extension in Taiwan's pre-collision zone: a new model of plate-bending in continental crust. Geology 40, 831–834. http://dx.doi.org/10.1130/G33142.1.

Lin, A.T., Watts, A.B., Hesselbo, S.P., 2003. Cenozoic stratigraphy and subsidence history of the South China Sea margin in the Taiwan region. Basin Res. 15, 453–478. http://dx.doi.org/10.1046/j.1365-2117.2003.00215.x.

Lu, C.Y., Hsu, H.J., 1992. Tectonic evolution of the Taiwan Mountain Belt. Petrol. Geol. Taiwan 27, 21–46.

Riedel, W., 1929. Zur Mechanik Geologischer Brucherscheinungen. Zentralbl. Miner. Geol. Palaontol. B 354–368.

Snoke, J.A., Munsey, J.W., Teague, A.C., Bollinger, G.A., 1984. A program for focal mechanism determination by combined use of polarity and SV–P amplitude ratio data. Earthq. Notes 55 (#3), 15.

Teng, L.-S., Wang, Y., Tang, C.-H., Huang, C.-Y., Huang, T.-C., Yu, M.-S., Ke, A., 1991. Tectonic aspects of the Paleogene depositional basin of northern Taiwan. Proc. Geol. Soc. China 34, 313–336.

Tsan, S.F., 1971. Structural geology of the southern Hsuehshan Range, Taiwan. Proc. Geol. Soc. China 14, 62–75.

Twiss, R.J., Moore, E.M., 1992. Structural Geology. W.H. Freeman and Company, p. 532.

Waldhauser, F., Ellsworth, W.L., 2000. A double-difference earthquake location algorithm: method and application to the northern Hayward fault, California. Bull. Seismol. Soc. Am. 90, 1353–1368.

Wu, F.T., 1978. Recent tectonics in Taiwan. J. Phys. Earth 26, 265–$299.

Wu, F.T., Chang, C.S., Wu, Y.M., 2004. Precisely relocated hypocenters, focal mechanisms and active orogeny in Central Taiwan. Aspects of the tectonic evolution of China. Geol. Soc. Lond. Spec. Publ. 226, 333–353.

Wu, F.T., Liang, W.-T., Lee, J.-C., Benz, H., Villasenor, A., 2009. A model for the termination of the Ryukyu subduction zone against Taiwan: a junction of collision, subduction/separation, and subduction boundaries. J. Geophys. Res. 114, B07404. http://dx.doi.org/10.1029/2008JB005950.

Wu, F.T., Kuo-Chen, H., McIntosh, K., 2014. Subsurface imaging, TAIGER experiments and tectonic models of Taiwan. J. Asian Earth Sci. http://dx.doi.org/10.1016/j.jseaes.2014.03.024.